Assessment indexes for converter p-Q control coupling

energies

MDPI

Article

Assessment Indexes for Converter P-Q Control Coupling

Panagis N. Vovos [1,*], Ioannis D. Bouloumpasis [2] and Konstantinos G. Georgakas [3]

[1] Department of Electrical and Computer Engineering, University of Patras, Rio Campus, 26504 Patras, Greece
[2] Department of Electrical Engineering, Chalmers University of Technology, 41296 Gothenburg, Sweden; ioannis.bouloumpasis@chalmers.se
[3] Department of Electrical and Computer Engineering, University of the Peloponnese, 26334 Patras, Greece; kgeorgakas@uop.gr
* Correspondence: panagis@upatras.gr; Tel.: +30-2610-969-866

Received: 11 February 2020; Accepted: 27 February 2020; Published: 3 March 2020

Abstract: This work presents a concise methodology for the calculation of assessment indexes regarding the coupling between active and reactive power control observed on distribution level converters. First, the reader is introduced to the concept of power coupling; when, where and how it appears in power control of converters. A brief summary of the theory and formulation behind it is also included, together with relevant literature. Then, the methodology for the assessment of active and reactive power control performance of any grid-connected converter is presented. The impact of small control disturbances during a testing procedure is monitored, analyzed and converted to meaningful indexes, so that the type and level of coupling is quantified without putting the converter or the grid at risk. The efficiency of the methodology to assess the type and level of coupling is verified experimentally. This is done by assessing several power control approaches with different level of decoupling efficiency on the same power converter connected to a distribution grid. While the assessment is performed with safe, minimal disturbances, its exceptional accuracy is later confirmed by the level and type of coupling observed during significant power step changes.

Keywords: active and reactive power control; power coupling; power distribution lines; power electronics converters; power generation control; performance evaluation

1. Introduction

Distributed Generation (DG) penetration in distribution networks causes significant technical and operational issues, besides important energy market changes [1]. The most important issues are the reduced power quality, low inertia, decreased fault levels and power control instability. They rise from the fact that "heavy" prime movers and synchronous generators found in most traditional generation units are replaced with Renewable Energy Sources (RES), or generally DGs, interfaced to the grid with "light" power electronic converters. In addition, the point of connection of RES to the grid is mainly at the distribution level, rather than the transmission network. Thus, the direct implementation of traditional control techniques (active power controlled by frequency and reactive power controlled by voltage) cannot usually work efficiently due to different feeder properties.

This work focuses on this last issue concerning active (P) and reactive (Q) power control of DG converters, commonly mentioned in bibliography as P-Q coupling. The problem appears as simultaneous output P-Q oscillation after abrupt local load changes or changes of P and/or Q output setting of the DG unit. The oscillations may significantly affect power quality (grid voltage pattern, frequency, etc.), power allocation among the DGs or even lead to DG unit disconnection under certain

conditions. *P*-*Q* coupling affects both operational stability and economic efficiency of distribution grids with high penetration of DGs, such as the microgrids [2].

Initially, engineers found the practical solution of adding large inductors between the converter and the distribution grid, directly reinforcing the weak inductive nature of low voltage networks. However, this is an expensive solution, which also increases line voltage drop. Therefore, research now focuses on control methods that would alleviate the effects of *P*-*Q* coupling, with minimal or no additional hardware [3]. The extensive literature about suggested solutions can be roughly divided into three approaches. The first is based on transformation matrices that adjust the measured output voltage or power flow components according to the line impedance angle, before they become control inputs to a traditional controller [4–6]. The second approach introduces a voltage drop through converter modulation, as if there was an impedance added to the converter output, virtually making the properties of the distribution grid more inductive [7–9]. The third approach assumes that the distribution grid where the converter is connected has dominant resistive properties. Thus, sufficient control can be achieved if the measured output power components are swapped before they become input to traditional generation control, i.e., *P* is controlled by voltage and *Q* is controlled by frequency [10,11].

The effectiveness of the aforementioned approaches to tackle *P*-*Q* coupling is demonstrated by comparison of the improved control performance with traditional generation control or other previous approaches. However, the comparison is subjective, based on human-eye observations of monitored *P*-*Q* coupling oscillations, usually during sudden load or control set point changes. Little research has focused on providing some concise method of quantifying the extent and qualitative properties of coupling, so that different control methods can be compared. In [12,13], the authors created small signal models that predict root trajectories as *P* and *Q* control parameters change. The models did show a correlation between those parameters and *P*-*Q* control dynamic performance. However, they did not calculate any indexes that quantify control performance for different sets of parameters, neither produced any qualitative signals that indicate in which sense one performance is better than another. The authors of [14], use errors between *P*-*Q* dynamic performance and active and reactive power set points in order to improve control properties. However, they do not examine if there is any correlation between those errors and some kind of *P*-*Q* control performance benchmarking. In [15], a closed loop state-space model is used for the interpretation of active power oscillations, observed during *P*-*Q* control coupling for load sharing DGs. Although this work draws a connection between control input disturbances and transient performance, it does not specify the way this connection can be formulated in order to be used for performance assessment or comparison between performances. Finally, in [16], the authors formulate coupling as a function of control parameters. However, the calculation is valid only for a specific control method, assuming known network and control parameters, and does not provide any qualitative indexes for the comparison of similar magnitudes of coupling resulting from different sets of control parameters.

The main contribution of this work can be summarized to the following points:

- Development and demonstration of a specific control testing methodology that produces measurable indexes for the most important coupling characteristics of the control approach.
- Exploitation of these indexes for more accurate comparison between methods; i.e., not only assessing if a control method achieves some level of decoupling, but also how well this decoupling works.
- The suggested methodology is indifferent of converter technology and control approach as it is based on experimental measurements of provoked disturbances, which means that DG control specifications could be based on some or a combination of those indexes in the future.
- Coupling assessment is an important procedure, especially in distribution level application, due to the resistive nature of low voltage grids. An index-based measurable coupling assessment will be a significant tool regarding the investigation of the suitability of both software (control methods) and hardware (converter technology) in grid-connected applications. The proposed methodology

about coupling evaluation could act as a guideline about the control method and the suitability of the technology used in each application.

- The proposed coupling assessment method allows users to safely evaluate their setup performance with respect to coupling, before the beginning of the actual application. Thus, this paper should be considered as a first step towards the standardization of software and hardware adequacy (in terms of power coupling) in distribution level applications.

It should be clarified that this work does not provide any novel control method for *P*-*Q* coupling alleviation in distribution grids. Moreover, it is not the scope of the paper to determine which method or converter topology is most suitable regarding lower *P*-*Q* coupling in distribution network applications. The main scope of this work is to provide users with a robust tool regarding the secure and reliable evaluation of different control methods efficiency to tackle *P*-*Q* coupling in distribution level.

The remaining of this paper is structured as follows: in Section 2, the reason for with the *P*-*Q* decoupling control used on traditional generation units connected to transmission networks cannot be directly used for DG is briefly explained. Then, the importance of the DG units to mimic, as closely as possible, the *P*-*Q* control behavior of larger generation units connected to transmission networks is illustrated. The assessment indexes calculated from the suggested methodology in Section 3, actually describe the level of mimicking achieved by the control approach of the DG converter. In Section 4, the methodology is experimentally tested on a series of different power control approaches implemented on a low power converter connected to a distribution grid. Finally, conclusions about the efficiency of the suggested methodology to assess *P*-*Q* coupling, together with possible future extensions of this work, are included in Section 5.

2. P-Q Decoupled Control

The power flow from any generator to an infinite bus via a feeder is described by the following set of equations:

$$P = \left[\left(E{\cdot}V{\cdot}\cos\Delta - \mathrm{V}^2\right){\cdot}\cos\theta + E{\cdot}V{\cdot}\sin\Delta{\cdot}\sin\theta\right]/Z, \quad (1)$$

$$Q = \left[\left(E{\cdot}V{\cdot}\cos\Delta - \mathrm{V}^2\right){\cdot}\sin\theta - E{\cdot}V{\cdot}\sin\Delta\cos\theta\right]/Z, \quad (2)$$

where $\underline{E/\Delta}$ and $\underline{V/0^0}$ are the generator and infinite bus voltage phasor, respectively, and $\underline{Z/\theta}$ is the impedance of the feeder. The infinite bus voltage and the feeder impedance are assumed to be constant; a reasonable assumption for the timeframe of the analysis and measurements of the suggested method.

For a transmission line, $\theta \approx 90°$, so Equations (1) and (2) are approximated by Equations (3) and (4), respectively.

$$P = (E{\cdot}V/Z){\cdot}\sin\Delta, \quad (3)$$

$$Q = (E{\cdot}V/Z){\cdot}\cos\Delta - \left(V^2\right)/Z. \quad (4)$$

Since Δ is generally small, $\sin\Delta \approx \Delta$ and $\cos\Delta \approx 1$, so Equations (3) and (4) can be approximated further by Equations (5) and (6), respectively.

$$P \approx (E{\cdot}V/Z){\cdot}\Delta, \quad (5)$$

$$Q \approx V{\cdot}(E - V)/Z. \quad (6)$$

Equation (5) describes a stronger dependence of P from Δ than P from E. The deviation of E from the nominal value is kept relevantly small (for operating purposes), so its impact on P is practically insignificant in comparison with Δ. Therefore, it can be assumed that EV/Z can be approximated by a constant in Equation (5), making P proportional to Δ. On the other hand, Q is clearly a proportional function of E according to Equation (6). The linear relationships $P(\Delta)$ and $Q(E)$ are the foundation of traditional power control of large generation units connected to the transmission network. It is called "decoupled *P*-*Q* control", because each power component can be controlled independently. A change

of generator's mechanical input changes the rotational speed and Δ, thus, affecting mainly output P. A change of generator's voltage, by changing field current of synchronous generators, mainly affects output Q. Decoupled control is also assisted by the much bigger time constant of the $P(\Delta)$ control loop, mainly due to the physical inertia existing to the prime mover of the generator and the generator itself.

In practice, simple droop functions are used for the implementation of the independent control of each power component. In Equation (7), as long as there is a difference between requested (P_{set}) and measured (P_m) generated P, a proportional difference is created between targeted (f_{set}) and measured (f_m) frequency of the generator. Similarly, in Equation (8), a difference between requested (Q_{set}) and measured (Q_m) generated Q, causes a proportional difference between targeted (E_{set}) and measured (E_m) generation voltage.

$$f_m - f_{set} = K_P \cdot (P_m - P_{set}), \tag{7}$$

$$E_m - E_{set} = K_Q \cdot (Q_m - Q_{set}), \tag{8}$$

where K_P and K_Q are positive constants expressing the requested speed of recovery for P and Q, respectively. They are empirically limited to values less than 5%, so that the speed of recovery does not create control stability issues.

However, this control approach cannot be directly applied on distribution grids, simply because the assumption $\theta \approx 90°$, which simplified Equations (1) and (2) to Equations (3) and (4) does not hold. This means that P and Q remain functions of both f and E and the control cannot be so easily "decoupled". However, rotating generators in distribution grids have to mimic the control response of their larger counterparts, in order to maintain compatible operation during sudden load or generation changes. Furthermore, similar P control among all generation units assists the appropriate response to economic dispatch [17]. Q-V control also has to be applied system-wide, even if it may have different objectives on transmission and distribution level: maintaining voltage stability [18] and reducing reactive power flows [19], respectively.

Research efforts do consider the physical coupling between power components in distribution grids, but focus on developing control methods which make DGs respond as closely as possible to their larger rotating counterparts in transmission networks. The purpose of this paper is not to develop new control methods, neither to compare nor to validate existing methods. This paper aims to provide an assessment tool that can quantify the distance between the response of any DG power converter and the control target set by the required $P(f)-Q(E)$ decoupling described above. In the next section the theory for calculating a set of indexes for this purpose is presented, which can be calculated in simulation or experimental environment.

3. Assessment Indexes

In this Section, four indexes will be calculated for the level of decoupling achieved by any DG converter control method. The first two assess the ability of the converter to mimic the $P(f)$ and $Q(E)$ relationship observed by synchronous generators connected to transmission networks. Essentially, these indexes evaluate in what extent the tested control method follows the almost ideally decoupled behavior of transmission level rotating generators. As explained in Section 2, as closely to linearity the $P(f)$ and $Q(E)$ relationships are, the better the level of decoupling is. The last two estimate the impact that a change of the one power component has on the other (i.e., measure the change that a reactive power alteration will bring to active power and vise-versa). Ideally, a change in one power component will not affect the other. Thus, the smaller these indexes are the better the performance of the tested method is regarding P-Q coupling. All indexes are calculated assuming that perfectly decoupled control would accurately mimic the response of synchronous generators connected to transmission networks.

3.1. Index for the Assessment of P(f) Relationship

If the converter control achieves perfect decoupling between control quantities, as in transmission networks, then Equation (5) is valid. An alteration of Δ will cause a proportional change to P:

$$\Delta P = E \cdot V \cdot \Delta\Delta / Z. \tag{9}$$

Since, perfect mimicking of control requires identical response, Equation (7) also holds. Therefore, an error input $e_P = P_m - P_{set}$, at time t would cause a proportional deviation of generation frequency by $\Delta f = f_m - f_{set}$:

$$\Delta f(t) = K_p \cdot e_P(t) \tag{10}$$

However, the integration of f in time creates an angle Δ. If f changes by Δf, Δ is also expected to change by $\Delta\Delta$:

$$2\pi \int f(t)dt = \Delta \Rightarrow 2\pi \int \Delta f(t)dt = \Delta\Delta. \tag{11}$$

By substituting Δf in Equation (11) with Equation (10), and replacing $\Delta\Delta$ in Equation (9):

$$\Delta P = (2\pi \cdot K_P \cdot E \cdot V / Z) \int e_P(t)dt. \tag{12}$$

Now, assuming that the time frame T_s between the measurement of e_p and the control decision is small (e.g., the sample time of a Digital Signal Processor (DSP) implementing the control method) the resulting ΔP can be calculated as below:

$$\Delta P = A_P \cdot e_P, \text{ where } A_P = 2\pi \cdot K_P \cdot E \cdot V \cdot T_s / Z \tag{13}$$

Please note that, since π, K_p, E, V and Z are constant, A_P is also constant, as long as there is perfect decoupling (i.e., E is not affected by ΔP). Therefore, if we measure several different values of e_p at the input of the controller and the resulting values of ΔP at the converter's output, we expect the plot of the pairs to lie in a linear zone with slope given by Equation (13). On the contrary, scattered pairs of values mean either that power coupling is strong (E is affected by ΔP) and/or the assumption that P is proportional to Δ is not strong (see Section 2). However, the value of A_P is not known, as the internal structure of the controller (expressed here roughly by K_P) is also considered unknown. Thus, the slope of the expected plot is also not known in advance.

We suggest the following methodology for the calculation of an index that quantifies the level of controller's success to mimic $P(f)$ relationship noticed at generators connected to transmission level, even if the control method is unknown. Under normal operating conditions, i.e., no significant grid voltage disturbances or outages, we first plot the (e_p, ΔP) pairs for a wide range of e_p values. Then we use linear regression to define a line that best fits those pairs. The calculation of the averaged norm of residuals (*NoRavP*), defined as the norm of residuals divided by the number of pairs, gives an index for the $P(f)$ performance of the controller. The closer the value of *NoRavP* is to zero, the better the mimicking of the $P(f)$ response of a synchronous generator connected to a transmission network is and vice versa. Thus, the index *NoRavP* will be calculated as:

$$NoRavP = \left[\sum_{i=1}^{N} \sqrt{\left(\Delta P_{m,i}^2 - \Delta P_{l,i}^2 \right)} \right] / N, \tag{14}$$

where $\Delta P_{m,i}$ is the measured active power change at converter output for the respective $e_{p,i}$ and $\Delta P_{l,i}$ is the calculated active power change at converter output from the linear regression for the same $e_{p,i}$, for a number N of measurements (i).

However, we have to emphasize that this index cannot provide a signal whether the imperfectness of $P(f)$ control is due to the inefficiency of the controller to maintain a linearity on $P(\Delta)$ or decouple E and P. The distinction is assisted by the additional indexes calculated in Section 3.3.

3.2. Index for the Assessment of Q(E) Relationship

Assuming perfect decoupling between control quantities makes Equation (6) valid for the ideal $Q(E)$ controller. Changing E will cause a proportional change to Q:

$$\Delta Q = V \cdot \Delta / Z \Leftrightarrow \Delta E = Z \cdot \Delta Q / V \tag{15}$$

Ideally, controller's response should follow Equation (8). An input error $e_Q = Q_m - Q_{set}$, would cause a deviation to output voltage by $\Delta E = E_m - E_{set}$:

$$\Delta = K_p \cdot e_Q \tag{16}$$

By substituting ΔE in Equation (15) by Equation (16) and solving with respect to ΔQ:

$$\Delta Q = A_Q \cdot e_Q, \text{ where } A_Q = K_Q \cdot V / Z \tag{17}$$

A_Q is constant (because K_Q, V and Z are constant) assuming perfect decoupling, i.e., f is not affected by ΔQ. As with the analysis for the P(f) relationship, if we measure different values of e_Q at the input of the controller and the resulting values of ΔQ at converter's output, we expect the plot of the pairs to lie in a linear zone with slope given by Equation (17). Otherwise, either power coupling is strong (f is affected by ΔQ) and/or the assumption that Q is proportional to E is not strong (see Section 2). As with A_P, the exact value of A_Q is not known, thus, the expected slope is also not known in advance.

The suggested methodology for the calculation of an index that quantifies the level of controller's success to mimic $Q(E)$ relationship found in transmission networks, is similar to the one suggested for $P(f)$. Under normal operating conditions we first plot the (e_Q, ΔQ) pairs for a wide range of e_Q values. Then we use linear regression to define a line with a slope that best fits those pairs. The calculation of the averaged norm of residuals (*NoRavQ*) gives an index for the $Q(E)$ performance of the controller. The closer the value of *NoRavQ* is to zero, the better the mimicking of the $Q(E)$ response of a synchronous generator connected to a transmission network is and vice versa. Thus, the index *NoRavQ* will be calculated as:

$$NoRavQ = \left[\sum_{i=1}^{N} \sqrt{\left(\Delta Q_{m,i}^2 - \Delta Q_{l,i}^2\right)}\right] / N, \tag{18}$$

where $\Delta Q_{m,i}$ is the measured reactive power change at converter output for the respective $e_{q,i}$ and $\Delta Q_{l,i}$ is the calculated reactive power change at converter output from the linear regression for the same $e_{q,i}$, for a number N of measurements i.

As with *NoRavP*, *NoRavQ* cannot provide information whether poor $Q(E)$ control performance is due to poor linearity of $Q(E)$ or decoupling between f and Q. That is why additional indexes are calculated in Section 3.3.

3.3. Indexes for Coupling Assessment of P with Q and Q with P

In the previous subsections two assessment indexes for the capability of the controller to mimic the $P(f)$ and $Q(E)$ control of generators connected to transmission networks were defined. However, it was stressed that bad indexes may be the result of either power coupling or lack of linearity between control input and output. In this subsection a methodology for the calculation of two more indexes that quantify the extent that each factor affects controller's performance are suggested.

Both new indexes measure the level of power coupling suffered by the controller under assessment. Having this information, the extent of non-linearity for $P(f)$ and $Q(E)$ control, using the information provided by the previous two indexes for the overall performance of the controller can be determined. For an ideal controller a disturbance at one power component should not have any impact to the other, assuming a decoupled and steady state operation before the disturbance. We can measure the level of

imperfection for any controller if we cause disturbances only at one power component and measure the impact on the other.

Actually, no additional tests should be run on the converter, because the data provided during the calculation of *NoRavP* and *NoRavQ* can be used. More specifically, by making step changes to P_{set} and keeping Q_{set} constant, we monitor e_p and ΔP for the calculation of *NoRavP*, but we also monitor the impact e_p has on e_Q because of control coupling. The RMS value of e_Q averaged by the number of data points provides an index (*SeQ*) of how much *P* affects *Q* due to control coupling. Similarly, index *SeP* is an index of how much *Q* affects *P*, and it can be calculated during *NoRavQ* evaluation by step changes of Q_{set}.

3.4. Conditions for Secure and Reliable Calculation of Indexes

The purpose of this subsection is to clarify the test procedure required for the calculation of the aforementioned indexes. The procedure does not require any knowledge about the control method or parameters used by the converter. It actually measures the response differences between the converter under assessment and an ideal converter behaving as a synchronous generator connected to a transmission network. Specifically, assessment indexes (*NoRavP, NoRavQ, SeQ, SeP*) are calculated according to the response of the converter to the control inputs, only. This response is compared to an ideal, perfectly decoupled response, formulated in Equations (9)–(13) and Equations (15)–(17), which also does not require any knowledge of the control approach under assessment. However, the assessment process requires access to controller's power set points (to create disturbances) and input signals (to measure response).

It must be emphasized, that controller's response depends on the properties of the system, where the converter is connected. For example, simple droop control may present as good indexes as any sophisticated control, when the converter supplies power to a highly inductive line. The superiority of better control will be measurable if tested on a common distribution grid (line R >> X). Therefore, if different converters or different controllers on the same converter have to be assessed it must be done under the same conditions. All assessment tests have to be run on the same or similar feeder and when there are no significant grid disturbances at the time of assessment. Practically, it cannot be said that one control is better than the other, if the conditions are not first specified.

Furthermore, a strong power source has to supply the required power; for example, a regulated dc power supply must be the dc source for a dc/ac grid-connected inverter. Otherwise, supply-oriented disturbances, caused by RES volatility or V-I dependence, may change the impact of control-initiated disturbances. The instruments used for the measurement of electric quantities must be appropriate for the quality of supply during tests. Higher harmonics may affect readings on inappropriate power measuring equipment. The same method of measurement (e.g., for the calculation P) and, if possible, the same measuring equipment must be used across different assessments.

Finally, the disturbances to the input of each controller must be identical (in terms of magnitude and timing) between tests for different controllers, so that the comparison of results is possible. Due to the existence of coupling, bigger disturbances of one power component are expected to create bigger disturbances to the other and vice versa. Therefore, the controllers must be stressed with the same disturbances of power components in order to get comparable indexes.

Here, it should be clarified that this work aims towards the evaluation of different control methods regarding their coupling performance. Therefore, converter technology is kept constant throughout the experiments. Nevertheless, the proposed method does not rely on a specific converter technology and it should provide reliable conclusions regarding power coupling even when different converter technologies are compared. The verification of the proposed method's accuracy under different converter technologies will be the scope of future research.

4. Experimental Verification

In the previous Section, the suggested indexes have been calculated and their assessment properties have been described. The purpose of this Section is double: (a) to demonstrate, in practice, how these indexes can be calculated for a power converter and (b) to validate the assessment properties of the indexes, by matching *P*-*Q* control coupling expected from calculated indexes with "traditional" engineering sense for coupling. In order to achieve it, first, the experimental setup (source, converter, grid), including a summary of converter operation, will be briefly described. Then, three basic *P*-*Q* control decoupling methods will be assessed by calculating the suggested indexes. Finally, the coupling properties (or their absence) observed during abrupt power changes for each control method, will be interpreted using the calculated indexes.

4.1. Experimental Setup

In this work, the suggested assessment indexes using the setup presented in Figure 1 are experimentally verified. The description of converter's elements, grid characteristics and local load at the Point of Common Coupling (PCC) are included in Table 1. A 250 V/10 A laboratory power supply plays the role of V_{DC}. A dc power supply was used in this work for simplicity reasons. However, the proposed coupling evaluation methodology does not depend on the nature of the dc source. Therefore, the generality of the obtained results and the conclusions derived by them will not be significantly affected by the dc source. It is expected that even in the case of intermitted dc source at converter input (PV array, wind turbine, etc.) the resulting conclusions about the performance of the tested control methods will not be affected. In addition, grid resistance and inductance values match the ones of the local distribution grid and have been estimated according to experimental measurements [20]. As a result of the relatively high dc voltage level, a step-up transformer is not necessary. Instead, a 1:1 isolation transformer is used for safety reasons

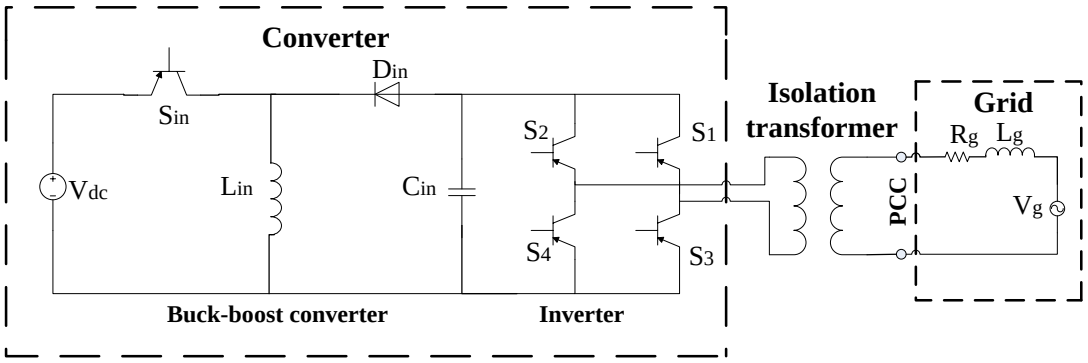

Figure 1. Schematic of experimental setup.

Table 1. Values of the setup characteristic elements.

Quantity	Symbol	Value/Model
Buck-boost converter inductance	L_{in}	1 mH
Buck-boost converter capacitance	C_{in}	10 μF
Buck-boost converter switching frequency	f_{bb}	20 kHz
Inverter Switching frequency	f_{inv}	50 Hz
Grid line inductance	L_g	1.187 mH
Grid line resistance	R_g	1.35 Ω
Buck-boost converter IGBT	S_{in}	FGL35N120
Inverter IGBTs	$S_1 - S_4$	FGL35N120
Buck-boost converter diode	D_{in}	DSEI60-10A

V_{DC} is fed to a buck-boost converter that operates at high frequency (here, 20 kHz). Buck-boost output voltage is a rectified sine waveform, having the same RMS value and frequency with grid voltage (230 V, 50 Hz). A detailed description of the modulation technique can be found in [21], which also allows harmonic current and voltage compensation. This voltage is fed to the full-bridge polarity swapping inverter that operates at grid voltage frequency. Inverter operation in low frequency is one of the major advantages exhibited by this topology, as it combines low harmonic content along with low switching losses [22]. Of course, neither converter technology nor modulation technique affects the calculation methodology of the assessment indexes (see Section 3).

4.2. Power Control Methods under Assessment

As it has already been underlined, the calculation of the assessment indexes is indifferent of the power control method used. Therefore, the indexes will be calculated for three control methods: conventional droop control, power transformation matrix and power transformation matrix with virtual resistor (this last hybrid method is fully explained in [23]). All control methods were designed with the MATLAB/Simulink platform and were implemented by the TI f28377d control card of the converter, using the setup describe in Section 4.1.

Figure 2 presents a generic flowchart that can accommodate all three power control methods under assessment. Measured converter voltage (V_m) and current (I_m) are the inputs. Using these measurements active (P_m) and reactive power (Q_m) are calculated as: $P_m = V_m \times I_m \times cos\theta$ and $Q_m = V_m \times I_m \times sin\theta$, where θ is the phase between the voltage and current fundamental components. Thus, it should be mentioned that reactive power control refers only to the control of the fundamental component of the reactive power. The calculated active (P_m) and reactive (Q_m) power pass through a low pass filter that creates a larger time constant for the $P(f)$ control loop, in order to assimilate the dynamics of a synchronous generator (see Section 2). Filter output is subtracted from the set values (P_{set}, Q_{set}), so that the input error is calculated for the controller (P_{err}, Q_{err}). Given a specific rotation angle, a transformation matrix converts the actual error P_{err}, Q_{err} to the modified error p_{err}, q_{err}. This is the input to a conventional droop controller, which converts p_{err}, q_{err} to deviations of converter frequency (Δf) and voltage amplitude (ΔV) from the measured grid values (f_g, V_g). At the last stage, a virtual resistor R_{virt} creates a virtual voltage drop ΔV_v, which is proportional to I_m. The resulting voltage signal is the one used for the modulation of the output voltage of the converter (V_{modul}).

With appropriate configuration of parameters, we can get all three control methods from the same generic flowchart. Setting $R_{virt} \neq 0$ and a non-zero rotation angle we get the control method of the Power Transformation Matrix with Virtual Resistor (PTMVR). If we short-circuit the virtual resistor ($R_{virt} = 0$), then $\Delta V_v = 0$ and the flowchart depicts the Power Transformation Matrix (PTM) control method. If we also set the rotation angle of the transformation matrix equal to zero, then the rotation matrix has no effect on the error signals ($P_{err} = p_{err}$ and $Q_{err} = q_{err}$) and the control is simplified to traditional droop.

Droop characteristics remain unchanged for all control methods. Specifically, $K_P = 0.0024$ and $K_Q = 0.00011$ (see Equations (7) and (8), respectively) for a DSP sample time of 0.0001 s. Table 2 contains the parameter settings for the control methods under assessment. It can be noticed that the control method of the PTMVR will be tested with two different sets of rotation angles and resistor values; the first one matches the characteristics of the grid, whereas, the second is randomly selected. For a more detailed description of each control method, please refer to the relevant literature mentioned in the introduction and references included within.

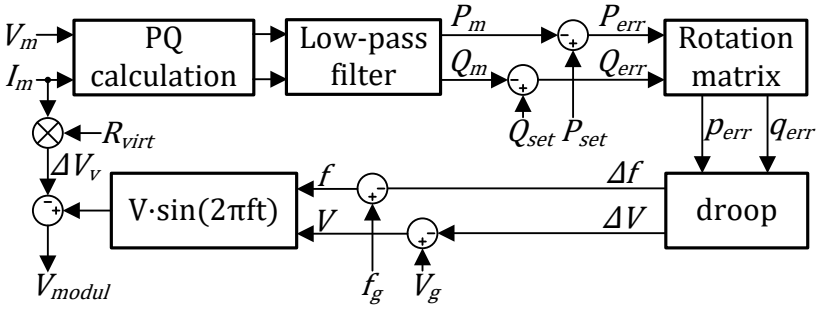

Figure 2. Generic flowchart for the power control methods under assessment.

Table 2. Configuration parameters of control methods under assessment.

Method	Rotation Angle (°)	R_{virt} (Ω)
Droop	0	0
PTM	64	0
PTMVR (matching grid)	88	10
PTMVR (random)	79	20

4.3. Experimental Process for the Calculation of Assessment Indexes

As it was explained in detail in Section 3.4, all indexes are calculated by measuring the impact of disturbances at controller's input set values on power output. Figure 3a presents the disturbance pattern of e_P by periodic step changes of P_{set} between P_{min} = 381 W and P_{max} = 508 W every Δt_P s, while Q_{set} was kept constant (0 Var). The choice of P_{min} and P_{max} is arbitrary. However, their difference has to be sufficiently small, so that even strongly coupled power control can be assessed, but the process itself cannot lead to instability. Δt_P depends on control speed and it is selected so that P_m barely reaches P_{set} ($e_P = 0$) before P_{set} changes again. This way the controller is permanently under disturbance conditions. Here, the control loop is implemented on a DSP, where a disturbance e_P in the current cycle (t) causes an alteration of real and reactive power, which is measurable in the next cycle ($t + 1/f_g$). This means that two pairs are practically recorded every cycle in the form:

$$[e_P(t),\Delta P(t)] = [P_m(t)\text{-}P_{set}(t),P_m(t + 1/f_g)\text{-}P_m(t)] \text{ for } NoRavP \text{ and}$$

$$[e_P(t),e_Q(t)] = [P_m(t)\text{-}P_{set}(t),Q_m(t + 1/f_g)\text{-}Q_{set}(t)] \text{ for } SeQ$$

Similarly, Figure 3b presents the disturbance pattern of e_Q by periodic step changes of Q_{set} between Q_{min} = −63 Var and Q_{max} = 63 Var every Δt_Q s, while P_{set} was kept constant at 508 W. These disturbances allow recording of pairs in the form:

$$[e_Q(t),\Delta Q(t)] = [Q_m(t)\text{-}Q_{set}(t),Q_m(t + 1/f_g)\text{-}Q_m(t)] \text{ for } NoRavQ \text{ and}$$

$$[e_Q(t),e_P(t)] = [Q_m(t)\text{-}Q_{set}(t),P_m(t + 1/f_g)\text{-}P_{set}(t)] \text{ for } SeP$$

The test procedure for all control methods lasted 90 s for real power disturbances and 90 s for reactive power disturbances. That amount of time gives a total of 90 s/20 ms = 4500 pairs of values for the calculation of each assessment index. Increasing the time of the test procedure beyond 90 s did not improve the calculated indexes significantly.

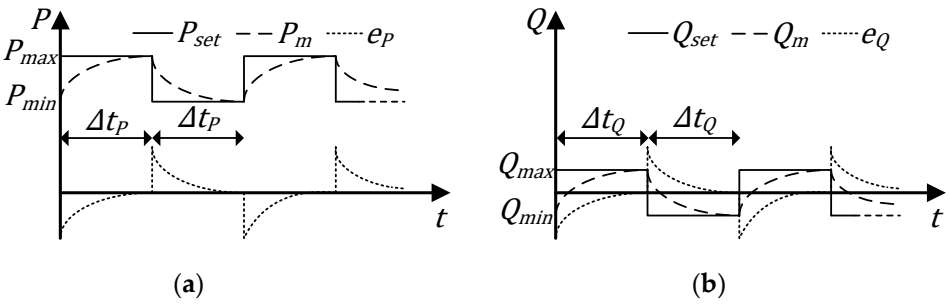

Figure 3. Controller disturbance pattern: (**a**) active power, (**b**) reactive power.

4.4. Assessment Results

A properly tuned power controller is expected to present both linear response and decoupled power components during disturbances (see Section 3). This assumption is verified from the experimental calculation of the assessment indexes for the power control methods under assessment (see Section 4.2). Figure 4 presents the plot of $[e_P(t), \Delta P(t)]$ pairs recorded for the PTMVR method configured properly in order to match grid characteristics. Linear regression of this data gives the straight line drawn on the same plot with *NoRavP* = 0.097. Figure 5 contains the same type of data, this time for conventional droop control. Clearly, plotted pairs are scattered in a much greater distance from the regression line, giving a much higher/worse *NoRavP* = 0.178. Figures 6 and 7 are the plots of $[e_Q(t), \Delta Q(t)]$ pairs for the properly configured PTMVR method and conventional droop control, respectively. Again, linear regression provides a much better *NoRavQ* for the PTMVR method (0.026 vs. 0.086 for droop control).

The *NoRavP* and *NoRavQ* indexes verify the expected superior power control performance of the PTMVR method for converters connected to distribution grids. The indexes show that it imitates the $P(f)$ and $Q(E)$ response of a synchronous generator connected to a transmission network much better than conventional droop control.

However, it is not clear how strong the coupling factor is for each of the two control methods. According to the arguments presented in Section 3.3, *SeP* and *SeQ* indexes are expected to signify how strong coupling exists between the power components. Figures 8 and 9 contain the $[e_P(t), e_Q(t)]$ pairs recorded for the PTMVR method with appropriate configuration and conventional droop control, respectively. From these plots it can be calculated that *SeQ* = 4.0 for the PTMVR method, a couple of orders lower than *SeQ* = 104.5 for droop control. Figures 10 and 11 contain the $[e_Q(t), e_P(t)]$ pairs recorded for the two methods. It can be calculated that *SeP* = 5.3 for the PTMVR method and *SeP* = 37.5 for droop control.

A comparison between *SeQ* and *SeP* indexes for the two methods demonstrates the ability of those two indexes to depict coupling of power components. Conventional droop control was expected to suffer from intense coupling when the converter is connected to a distribution grid, thus *SeQ* and *SeP* indexes are much worse.

Table 3 concentrates the aforementioned index values, plus, the index values which have been calculated for the PTM method and the randomly configured PTMVR method. A comparison of indexes between methods shows that a method may be better at some indexes, but worse at others. For example, PTM has better *NoRavQ* and *SeP* than PTMVR with random configuration, but it has worse *NoRavP* and *SeQ*. Obviously, there are cases that cannot be judged as better than other, if criteria are not defined first. The assistance of the indexes is crucial; if we are interested mostly on the $P(f)$ control loop, we should be focusing at *NoRavP* and *SeQ*, whereas, if we are interested on $Q(E)$, we should be looking mainly at *NoRavQ* and *SeP*.

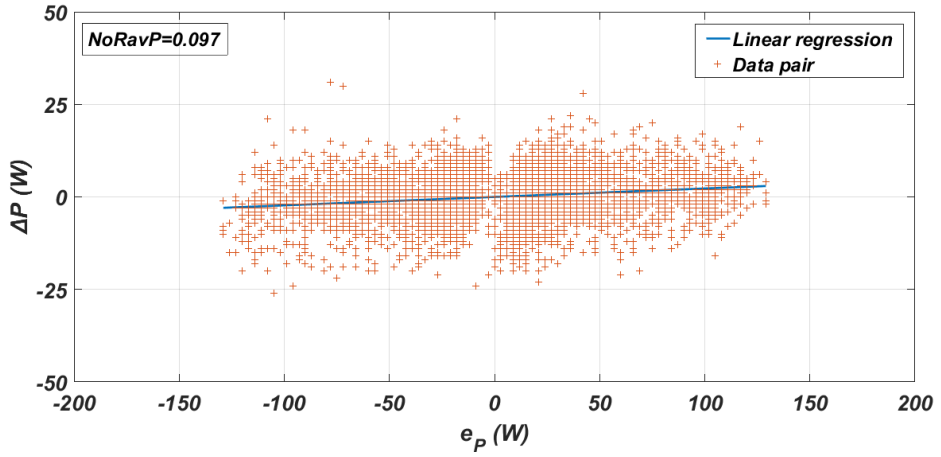

Figure 4. Plot and linear regression of $[e_P(t), \Delta P(t)]$ pairs used for the calculation of *NoRavP* for the properly configured Power Transformation Matrix with Virtual Resistor (PTMVR) control method.

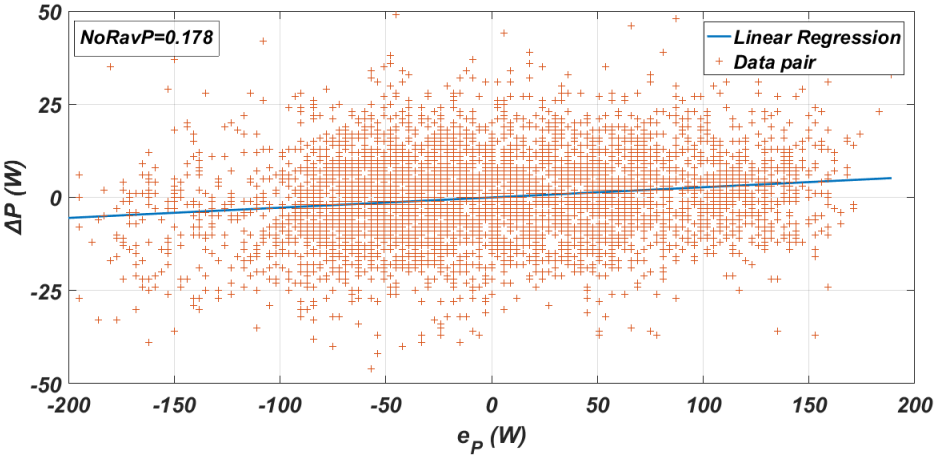

Figure 5. Plot and linear regression of $[e_P(t), \Delta P(t)]$ pairs used for the calculation of *NoRavP* for droop control.

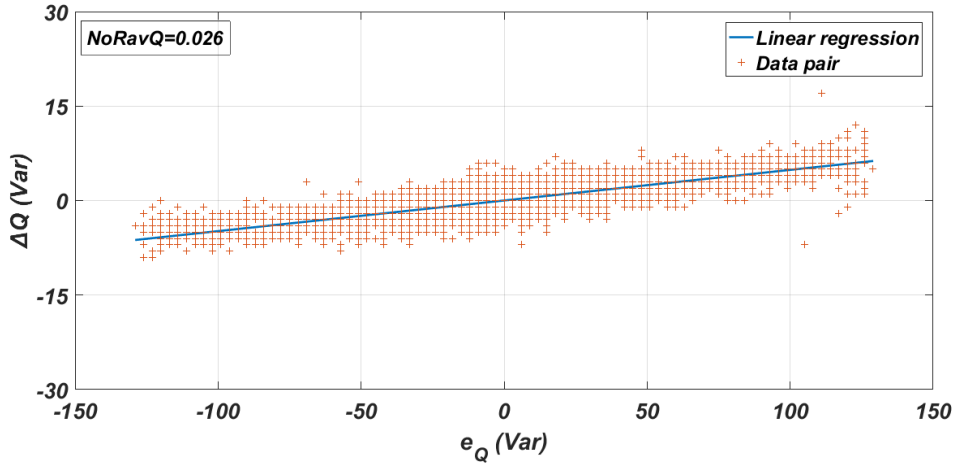

Figure 6. Plot and linear regression of $[e_Q(t), \Delta Q(t)]$ pairs used for the calculation of *NoRavQ* for the properly configured PTMVR control method.

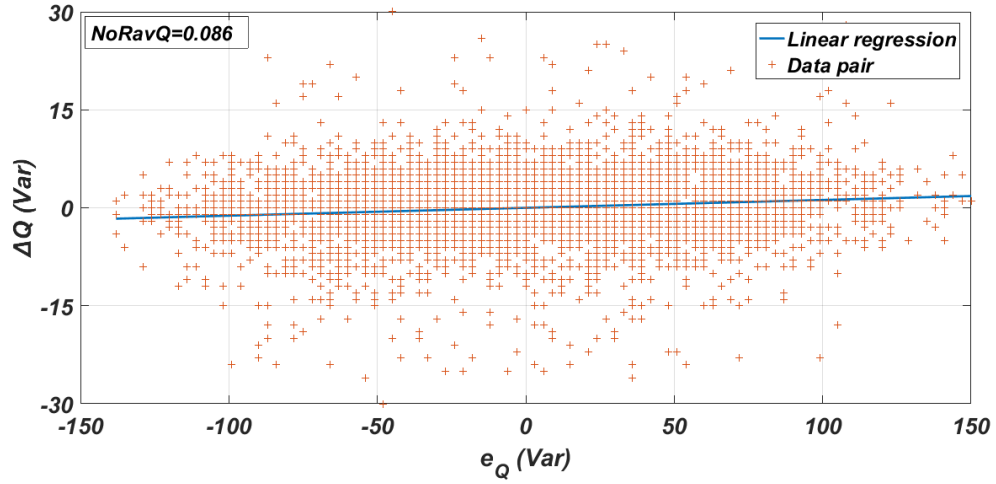

Figure 7. Plot and linear regression of [$e_Q(t)$, $\Delta Q(t)$] pairs used for the calculation of *NoRavQ* for droop control.

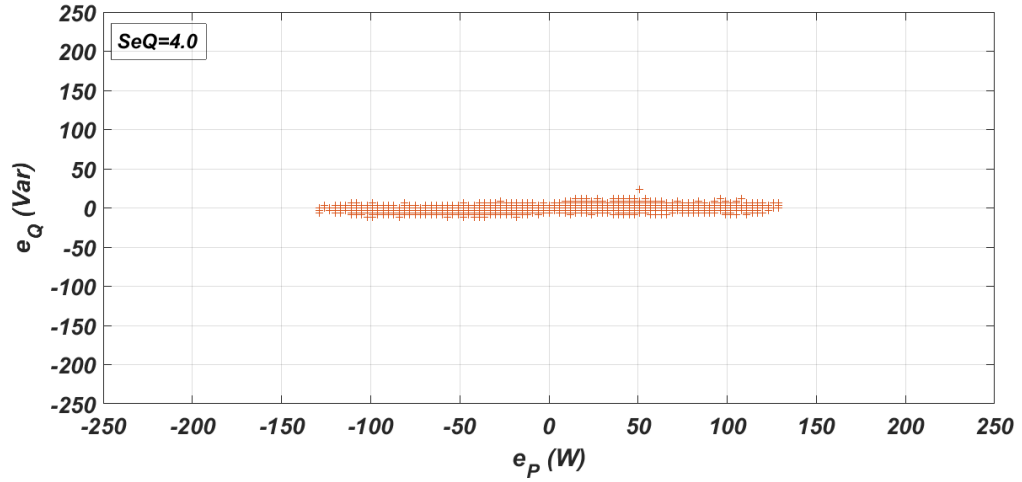

Figure 8. Plot of [$e_P(t)$, $e_Q(t)$] pairs used for the calculation of *SeQ* for the properly configured PTMVR method.

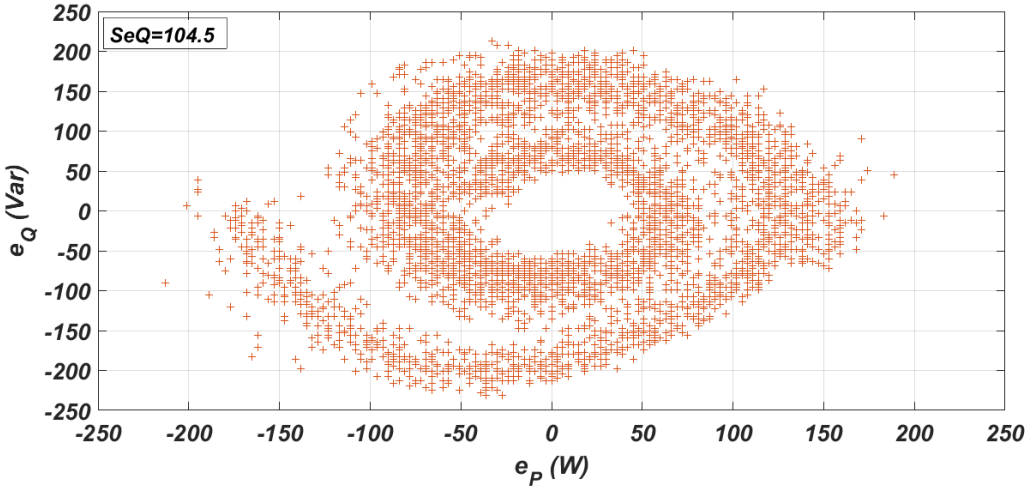

Figure 9. Plot of [$e_P(t)$, $e_Q(t)$] pairs used for the calculation of *SeQ* for droop control.

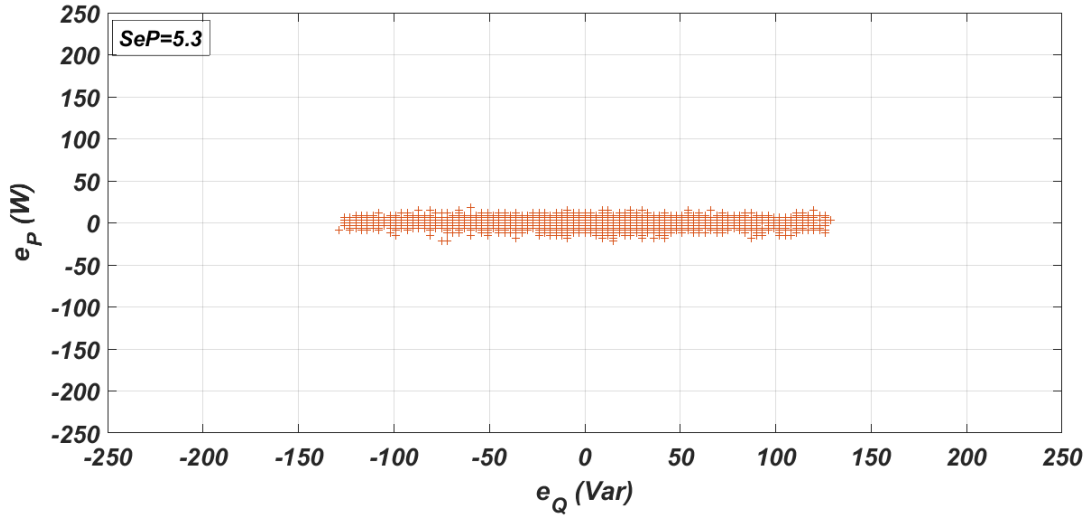

Figure 10. Plot of $[e_Q(t), e_P(t)]$ pairs used for the calculation of *SeP* for the properly configured PTMVR method.

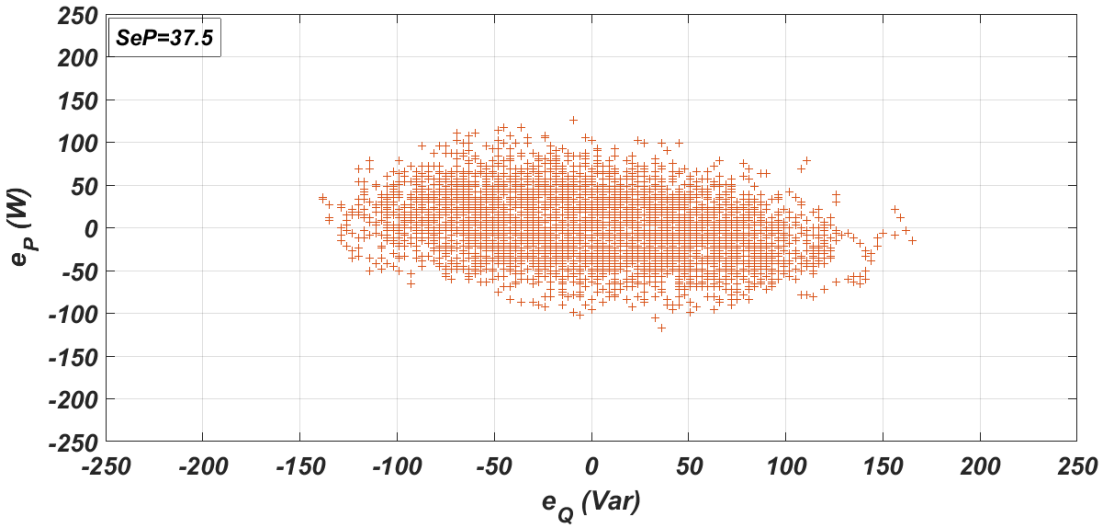

Figure 11. Plot of $[e_Q(t), e_P(t)]$ pairs used for the calculation of *SeP* for droop control.

Table 3. Index values for all control methods under assessment.

Method	*NoRavP*	*NoRavQ*	*SeQ*	*SeP*	*AVpu*
Droop	0.178	0.086	104.5	37.5	9.6
PTM	0.179	0.077	20.4	9.7	2.9
PTMVR (matching)	0.097	0.026	4.0	5.3	1.0
PTMVR (random)	0.108	0.094	8.8	12.0	2.3

Figures 12 and 13 present the response of the converter to large power step changes (200 to 800 W and −200 to 200 Var) utilizing the PTM and the PTMVR (random configuration) methods, respectively. This is a typical procedure in the literature, if a control method is to be tested for power coupling. Just comparing the two figures cannot possibly lead to a straightforward judgment if there is strong coupling or not for each method and, mostly, a comparison between the two responses cannot provide a unique answer on which is better. However, changes of P_{set} have lower impact on Q for the PTMVR

than the PTM method, which can be verified from the lower *SeQ* index. The reverse happens for changes of Q_{set}, where both response of *P* and *SeP* index is better for the PTM.

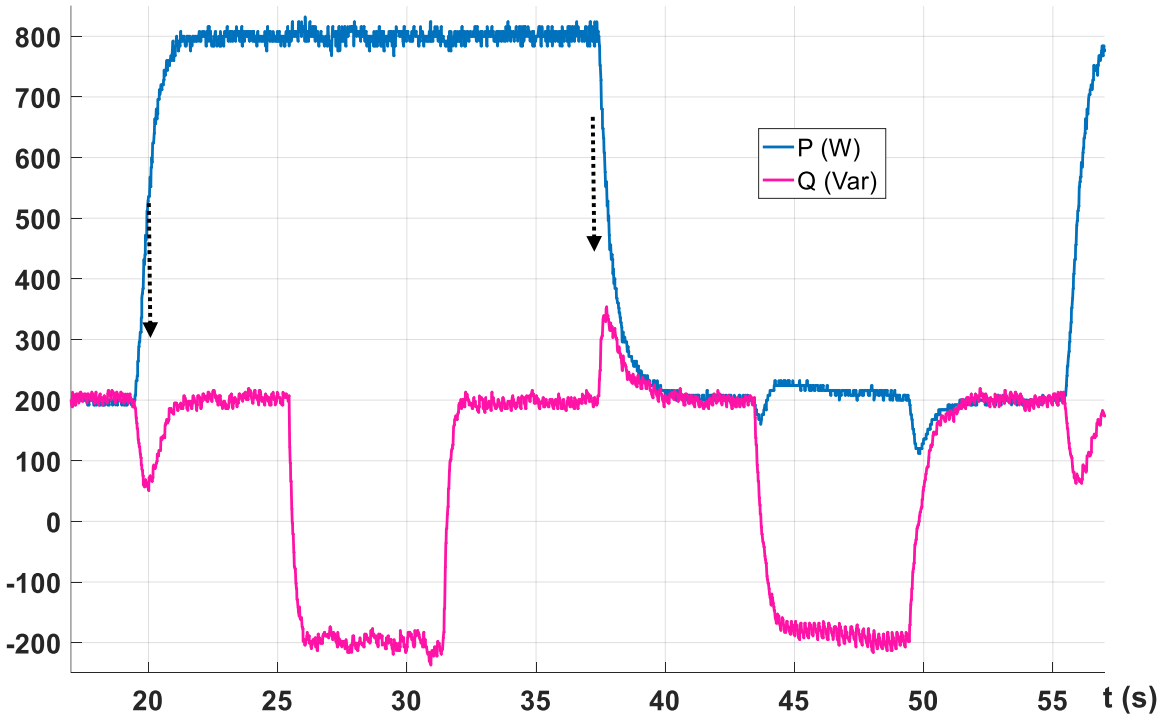

Figure 12. Response of Power Transformation Matrix (PTM) method to big step changes of P_{set} and Q_{set}.

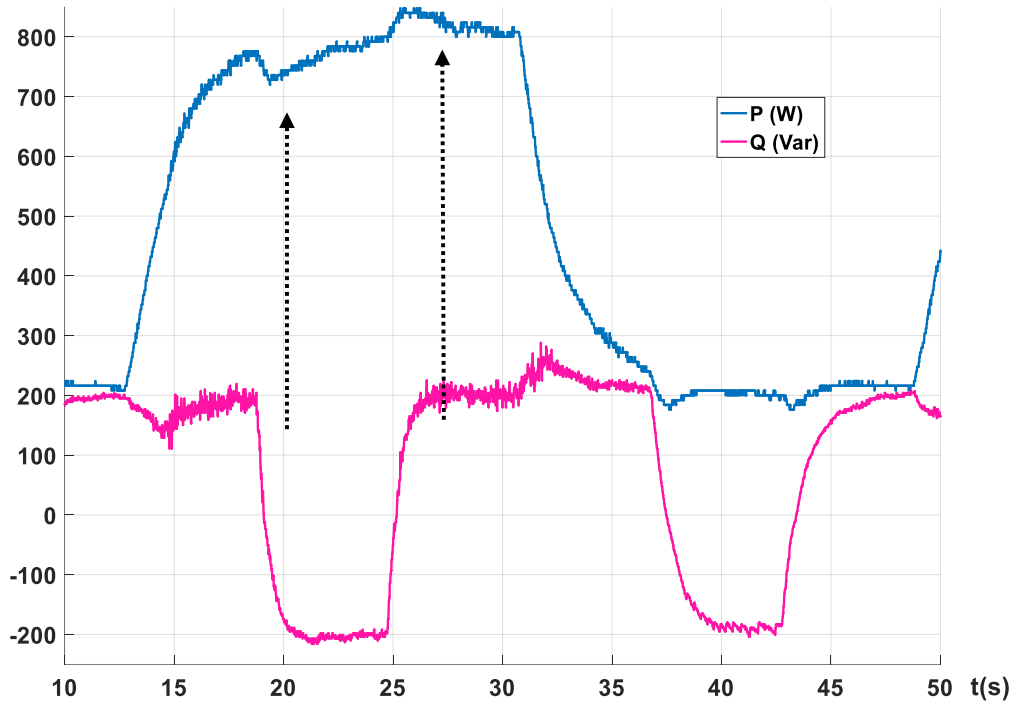

Figure 13. Response of PTMVR method (random configuration) to big step changes of P_{set} and Q_{set}.

Weighting factors for each index in a summation or more complicated function could determine the bias towards some of the assessment indexes. Here, we assumed that all control properties assessed

by the indexes have equal importance. Thus, each column of indexes in Table 3 is divided with the lowest/best value found in this column and then the average value of each row of indexes is calculated, creating a new overall index placed at the last column named *AVpu*. According to this new index, it can be verified that the properly configured PTMVR method presents weak power coupling properties, and the opposite happens for conventional droop control. As expected, PTM and randomly configured PTMVR have similar overall performance (*AVpu* = 2.9 vs. 2.3, respectively), so a better look has to be taken at specific indexes, depending on which criteria are considered more important.

5. Conclusions

This work aimed at specifying indexes for the coupling properties of power control methods used by converters connected to distribution grids. Four basic indexes were defined, based on a comparison between the ideal response of a synchronous generator connected to a transmission network and the control method under assessment. Practical aspects for the calculation of the indexes on real converters were also discussed. Different methods have been assessed experimentally, and the expected response has been verified and quantified from the calculated indexes. The indexes have also been proven a useful tool for the comparison of control methods with different power coupling properties, where the common approach of large step power disturbances cannot lead to definite conclusions. It is the target of future work to create a framework that will augment those indexes in a new standard or even provide the reference values and limits for future specifications on power control coupling of distribution converters.

Author Contributions: P.N.V. worked on the conceptualization and methodology for the calculation of the assessment indexes. He has also written the original draft for submission. I.D.B. and K.G.G. focused their work on experimental investigation and verification of presented theoretical analysis. All authors have worked on data curation, visualization and validation of results. All authors have read and agreed to the published version of the manuscript.

Funding: This research received no external funding.

Conflicts of Interest: The authors declare no conflict of interest.

References

1. Pepermans, G.; Driesen, J.; Haeseldonckx, R.B.D.; D'haeseleer, W. Distributed generation: Definition, benefits and issues. *Energy Policy* **2005**, *33*, 787–798. [CrossRef]
2. Wu, H.; Liu, Z.; Liu, J.; Wang, S. A Unified Virtual Power Decoupling Method for Droop-Controlled Parallel Inverters in Microgrids. *IEEE Trans. Power Electron.* **2016**, *31*, 5587–5603. [CrossRef]
3. Hossain, M.A.; Pota, H.R.; Issa, W.; Hossain, M.J. Overview of AC Microgrid Controls with Inverter-Interfaced Generations. *Energies* **2017**, *10*, 1300. [CrossRef]
4. De Brabandere, K.; Bolsens, B.; Van den Keybus, J.; Woyte, A.; Driesen, J.; Belmans, R. A Voltage and Frequency Droop Control Method for Parallel Inverters. *IEEE Trans. Power Electron.* **2007**, *22*, 1107–1115. [CrossRef]
5. Li, Y.; Li, Y.W. Power Management of Inverter Interfaced Autonomous Microgrid Based on Virtual Frequency-Voltage Frame. *IEEE Trans. Smart Grid* **2011**, *2*, 30–40. [CrossRef]
6. Rowe, C.N.; Summers, T.J.; Betz, R.E.; Cornforth, D.J.; Moore, T.G. Arctan Power–Frequency Droop for Improved Microgrid Stability. *IEEE Trans. Power Electron.* **2013**, *28*, 3747–3759. [CrossRef]
7. Li, Y.W.; Kao, C.N. An Accurate Power Control Strategy for Power-Electronics-Interfaced Distributed Generation Units Operating in a Low-Voltage Multibus Microgrid. *IEEE Trans. Power Electron.* **2009**, *24*, 2977–2988.
8. Zhang, P.; Zhao, H.; Cai, H.; Shi, J.; He, X. Power decoupling strategy based on 'virtual negative resistor' for inverters in low-voltage microgrids. *IET Power Electron.* **2016**, *9*, 1037–1044. [CrossRef]
9. Wu, X.; Shen, C.; Iravani, R. Feasible Range and Optimal Value of the Virtual Impedance for Droop-Based Control of Microgrids. *IEEE Trans. Smart Grid* **2017**, *8*, 1242–1251. [CrossRef]

10. Vandoorn, T.L.; Meersman, B.; de Kooning, J.D.M.; Vandevelde, L. Analogy between Conventional Grid Control and Islanded Microgrid Control Based on a Global DC-Link Voltage Droop. *IEEE Trans. Power Deliv.* **2012**, *27*, 1405–1414. [CrossRef]
11. Guerrero, J.M.; Berbel, N.; Matas, J.; de Vicuna, L.G.; Miret, J. Decentralized Control for Parallel Operation of Distributed Generation Inverters in Microgrids Using Resistive Output Impedance. In Proceedings of the IECON 2006—32nd Annual Conference on IEEE Industrial Electronics, Paris, France, 6–10 November 2006.
12. Ma, J.; Wang, X.; Liu, J.; Gao, H. An Improved Droop Control Method for Voltage-Source Inverter Parallel Systems Considering Line Impedance Differences. *Energies* **2019**, *12*, 1158. [CrossRef]
13. Lao, K.; Deng, W.; Sheng, J.; Dai, N. PQ-Coupling Strategy for Droop Control in Grid-Connected Capacitive-Coupled Inverter. *IEEE Access* **2019**, *7*, 31663–31671. [CrossRef]
14. Patel, U.; Gondalia, D.; Patel, H. Modified droop control scheme for load sharing amongst inverters in a micro grid. *Adv. Energy Res.* **2015**, *3*, 81–95. [CrossRef]
15. Jia, L.; Yushi, M.; Hassan, B. Enhanced Virtual Synchronous Generator Control for Parallel Inverters in Microgrids. *IEEE Trans. Smart Grid* **2017**, *8*, 2268–2277.
16. Yan, X.; Zhang, X.; Li, J.; Han, J. Inverter coupling evaluation and decoupling method based on dynamic relative gain. In Proceedings of the IEEE Transportation Electrification Conference and Expo Asia-Pacific, Harbin, China, 7–10 August 2017.
17. Li, N.; Zhao, C.; Chen, L. Connecting Automatic Generation Control and Economic Dispatch from an Optimization View. *IEEE Trans. Control Netw. Syst.* **2016**, *3*, 254–264. [CrossRef]
18. North American Electric Reliability Corporation. *Reliability Guideline—Reactive Power Planning*; NERC: Atlanta, GA, USA, 2016.
19. Szpyra, W.; Bąchorek, W.; Kot, A.; Makuch, A. Optimization Criteria for Reactive Power Compensation in Distribution Networks. *Acta Energetica* **2014**, *4*, 140–148. [CrossRef]
20. Asiminoaei, L.; Teodorescu, R.; Blaabjerg, F.; Borup, U. Implementation and Test of an Online Embedded Grid Impedance Estimation Technique for PV Inverters. *IEEE Trans. Ind. Electron.* **2005**, *52*, 1136–1144. [CrossRef]
21. Bouloumpasis, I.D.; Vovos, P.N.; Georgakas, K.G.; Vovos, N.A. Current Harmonics Compensation in Microgrids Exploiting the Power Electronics Interface of Renewable Energy Sources. *Energies* **2015**, *8*, 2295–2311. [CrossRef]
22. Bouloumpasis, I.D.; Vovos, P.N.; Georgakas, K.G.; Vovos, N.A. A Method for Power Conditioning with Harmonic Reduction in Microgrids. In Proceedings of the International Conference on Renewable Energy and Power Quality (ICREPQ' 14), Cordoba, Spain, 8–10 April 2014.
23. Heredero-Peris, D.; Pagès-Giménez, M.; Montesinos-Miracle, D. Inverter design for four-wire microgrids. In Proceedings of the 17th European Conference on Power Electronics and Applications (EPE'15 ECCE-Europe), Geneva, Switzerland, 8–10 September 2015.